

OPTIMAL DESIGN OF GEODETIC MONITORING NETWORKS BY MEANS OF INTERVAL MATHEMATICS

Steffen Schön¹ and Hansjörg Kutterer²

¹*Geodätisches Institut, Universität Karlsruhe (TH), Englerstrasse 7, D-76128 Karlsruhe Germany; e-mail: schoen@gik.uni-karlsruhe.de*

²*Deutsches Geodätisches Forschungsinstitut (DGFI), Marstallplatz 8, D-80539 Munich, Germany*

Abstract

Supposing normally distributed random measurement errors, in geodesy a least-squares adjustment is used to estimate the unknown parameters, i.e. typically the coordinates of geodetic networks. Due to atmospheric, topographic, or instrumental effects, corrections on the original measurements are applied before the adjustment process. Intervals can be used to describe the maximum uncertainty of the corrected observations coming from uncertainties of auxiliary measurements like, e.g., temperature or pressure, from instrumental imperfection or from model simplifications. Such intervals are assumed to contain all possible values. Hence an interval extension of the least-squares estimator describes the maximum uncertainty propagation from the preprocessed observations to the estimated parameters, i.e. the network coordinates. In this paper, the background of an interval-mathematically founded network analysis and optimization is presented. Some example intervals for electronic distance measurements as typical geodetic observations are derived. The impact of different network scenaria on the precision, reliability and interval criteria is shown numerically and is discussed.

1. Motivation

The determination of the Earth's surface is a fundamental task in geodesy. Often, parts of the surface of the Earth are represented by the coordinates of discrete points of geodetic networks. A *linear geodetic model* of the situation is obtained by linearizing the (in general) nonlinear relation between the unknown point coordinates (parameters) and the observations. The unknown parameters are estimated by means of a least-squares adjustment. Due to atmospheric, topographic, or instrumental effects, the mathematical description of the geodetic model expressing the observations as a function of the parameters is inconsistent with the physics which is actually valid for the measurements.

Hence, in order to keep the geodetic model as simple as possible and mathematically easy to handle, the observations have to be corrected by adequate *correction models*. Therefore, auxiliary recordings like temperature or pressure as well as other information are needed. Imperfection of these auxiliary measurements or imprecision of the information lead to new uncertainties of the corrected observations. Thus, *systematic effects* are corrected but remain to a certain amount. Regarding the treatment of these uncertainties, different approaches can be distinguished. First of all the influence of the correction step on the total error budget of the observations can be ignored. Hence only the noise of the original observations is considered which is described by the stochastic model. On the other hand, for the proper interpretation of the final results the simplifications have to be taken into account.

Alternatively, all effects coming from the correction models can be modelled by stochastic means by representing the models as functions of influence factors. The parameters, e.g. the auxiliary measurements or model constants, are understood as realizations of random variables and their

uncertainty as standard deviation, usually assuming a normal distribution. The expectation value equals the chosen correction model, whereas the variance-covariance propagation leads to correlated corrected observations. This approach is recommended by the ISO (1995).

The main criticism of the stochastic approach is directed to the assumption of the probability distribution. First, this assumption cannot be tested because of only one or a few readings for the auxiliary observations. More general, the statistic behaviour is not sufficiently determined. Furtheron, in technical realizations the set of all possible values is limited due to small and limited sensor imperfections. Taking these facts into account, it seems to be more appropriate to use non-stochastic approaches to describe imperfect knowledge. If we are interested in maximum effects of the uncertainty contributions of the correction models, a third, *interval-based approach* is adequate to model worst-case behaviour of the sensors. Then, information about the density distribution of the auxiliary measurements is not required.

In a first part of the paper, the concept of interval analysis is described. Using the example of electronic distance measurement, it is shown how interval radii can be derived. According to Kutterer (1994), the concept of least-squares adjustment is extended to the interval-based approach. Finally, a network optimization based on this new uncertainty concept will be presented.

2. Fundamentals of interval mathematics

In this section, some fundamentals of interval mathematics are presented which are necessary for the understanding of the following text. The basic reference is Alefeld and Herzberger (1983). In geodesy, Kutterer (1994, 1995) has studied these concepts.

A real *interval* $[a]$ is defined as a closed compact subset of the set of real numbers \mathfrak{R} and can be represented in two equivalent forms:

$$\begin{aligned} [a] &= [a_l, a_u] = \{ t \in \mathfrak{R} \mid a_l \leq t \leq a_u, a_l, a_u \in \mathfrak{R} \} \\ [a] &= \langle a_m, a_r \rangle, a_m \in \mathfrak{R}, a_r \in \mathfrak{R}_0^+ \end{aligned} \quad (1a,b)$$

where a_l denotes the lower and a_u the upper bound; a_m the interval midpoint and a_r its radius in the alternative representation, respectively. Figure No. 1 depicts the fundamental relation between these two representations given by Eq. (2).

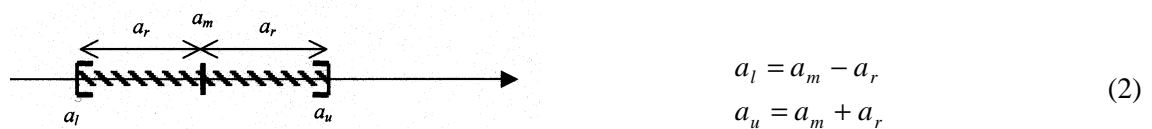


Figure No. 1: Interval representation

The elementary *arithmetic operations* are defined for intervals as results of the application of the corresponding real operations to all elements of the intervals. As a consequence subtraction is not inverse to addition, i.e. the midpoints are subtracted but the radii are added, cf. Eq. (3).

$$[a] - [b] = \langle a_m, a_r \rangle - \langle b_m, b_r \rangle \Rightarrow [a] - [a] = \langle a_m, a_r \rangle - \langle a_m, a_r \rangle = \langle 0, 2a_r \rangle \quad (3)$$

Addition and multiplication of intervals are associative and commutative operations. But the distributivity law is only valid in a generalized form (subdistributivity):

$$[a] ([b] + [c]) \subseteq [a] [b] + [a] [c] \quad (4)$$

The multiplication of an interval $[a]$ with a real scalar γ is given by:

$$\gamma [a] = \langle \gamma a_m, |\gamma| a_r \rangle \quad (5)$$

Real numbers are embedded as point intervals in the concepts of intervals. In this case, the lower and the upper bound are identical. Further, the concept of intervals can be extended to vectors of intervals and matrices of intervals. An *interval matrix* $[A]$ for example is a matrix where all elements are intervals.

The *interval extension of a real vector-valued function* f is defined by the substitution of the real vector x by the interval vector $[x]$:

$$f([x]) = \{ f(x) \mid x \in [x] \} \quad (6)$$

Two further properties have to be noted for interval vectors. The application of the real-valued linear matrix mapping $D = B C$ to an interval vector $[x]$ leads to an interval vector:

$$[y] = D[x] = \langle D x_m, |D| x_r \rangle \quad (7)$$

with the non-negative matrix $|D| = (|d_{ij}|) \geq 0$. The set of interval vectors is not closed with respect to mappings of type Eq. (7); the factual range of values is a convex polyhedron in general. The interval vector given by the first part of Eq. (8) represents the closest interval inclusion of this polyhedron. The subdistributivity yields

$$[y] = (B C) [x] \subseteq B (C [x]) \quad (8)$$

for all other evaluation sequences. Hence, the smallest interval inclusion can be reached only if the real matrix multiplication is done before the multiplication with an interval vector, cf. Kutterer (1995).

3. Interval-based description of uncertainty

In this section, interval-based quality measures are developed using the example of electronic distance measurement (EDM). In a first part, the necessity of corrections on the original observations is motivated. Then, different correction steps are presented. In a third part, interval radii as non-stochastic quality measures for the corrected observations are derived based on the sensitivity analysis of the correction models. Finally, concrete values will be given for the example of distance observations.

3.1 Geometric Relations

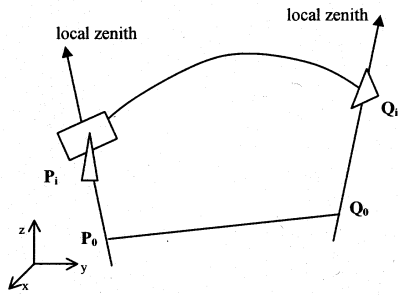


Figure No. 2: Geometric relations of the EDM

Figure No. 2 shows the situation for a distance between the two points P_i and Q_i measured by EDM. The geodetic model describes the Euclidean distance between P_0 and Q_0 . Hence corrections are necessary to correct the refracted ray $P_i Q_i$ to the Euclidean distance $D_0 = P_0 Q_0$ due to effects, like e.g., refraction, deflection of the vertical, choice of the reference system, or eccentricities caused by centering or instrumental heights.

3.2 Corrections Steps

Let D_I be the displayed distance value determined by the phase difference method, cf. Rüeger (1996, pp.15-21). It can be decomposed into three parts: the raw distance D_0 with the internal reference values n_0 for the refractive index, f_0 for the modulation frequency, c_0 for the velocity of light in vacuum. N denotes the ambiguities and $\Delta\phi$ the phase lead. Hence, the displayed distance value D_I contains *instrumental internal corrections*. Please note that the exact formulas used for these corrections in the instruments' software are not always published by the manufacturer.

$$\begin{aligned}
D_I &= \frac{c_0}{2n_0 f_0} \left(N + \frac{\Delta \varphi}{2\pi} \right) + d \left(\sqrt{n_p^2 - \sin^2 \beta} - n_p \right) + e(1 - \cos \beta) + a \\
&= D_0 \qquad \qquad \qquad + \Delta \qquad \qquad \qquad + a
\end{aligned} \tag{9}$$

The second part Δ takes into account the disorientation of the reflector, which occurs especially if the reflector is fixed, cf. R ueger (1996, pp.148-164). The height of the apex of the prism above the front surface is denoted by d , the offset of the vertical and horizontal axis from the front face by e , the angle of incidence by β , the refractive index of the prism material by n_p . Finally the additional constant is denoted by a .

In a next step, the displayed value D_I has to be corrected due to *atmospheric effects*. As an example we treat only the first velocity correction. The internal meteorological reference values, i.e. the temperature T_0 , the pressure p_0 , and the relative humidity h_0 , are used to compute the internal refractive index n_0 . They have to be replaced by representatively measured values, like e.g., T, p, h . Eq. (10) describes the atmospheric corrected distance D_A .

$$D_A = \frac{n_0}{n} D_I \tag{10}$$

The refractive index of the air n is derived according to the new IAG resolutions, cf. R ueger (1999). The needed saturation water vapour pressure is computed using the equation of Magnus-Tetens, cf. R ueger (1996, p.63).

Finally the *topographic corrections* from P_i to P_0 and Q_i to Q_0 are considered. Several effects occur like, e.g., the deflection of the vertical, the choice of the reference system, eccentricities of the instrumental reference. In this step it has to be noticed that a strict distinction between different measurement types, like e.g., distances, directions, zenith angles, or GPS measurements and a separate correction of each type of observation is not appropriate any longer. Correction models for one type of observations require other observations as input parameters. Hence, for a complete description, it is necessary to combine all measured polar elements (distance, direction and zenith angle) in a topocentric 3d Cartesian coordinate system.

3.3 Derivation of the interval radii as non-stochastic uncertainty measures

In the following we are interested in describing the impact of uncertainty of the different influence parameters \mathbf{p} in the correction models on the corrected observations, i.e. in our example the corrected distance D_A . In general two methods can be distinguished for this task. The first one is based on a *sensitivity analysis* of the correction models. Using the total differentials of Eqs. (9) and (10) yields:

$$dD_A = \frac{a + \Delta}{n} dn_0(T_0, p_0, h_0) - \frac{D_0 n_0}{n f_0} df_0 + \frac{n_0}{n} da + \frac{n_0}{n} d\Delta(d, e, n_p, \beta) - \frac{D_I n_0}{n^2} dn(T, p, h) + \delta \tag{11}$$

Hence, an appropriate linear relation between the corrected observation D_A and the various influence parameters, like e.g., the instrumental reference parameters T_0, p_0, h_0, f_0 , the auxiliary observations T, p, h , or the rounding-off error δ , is derived. Let \mathbf{f} denote the vector of partial derivations and $d\mathbf{p}$ the vector of differentials of the above-mentioned influence parameters. Then Eq. (11) can be represented in the following way:

$$dD_A = \mathbf{f}^T d\mathbf{p} \tag{12}$$

In order to manage worst-case sensor behaviour, the differentials $d\mathbf{p}$ have to be interpreted as maximum uncertainty of the corresponding influence factors. Furtheron, any contribution in the vector \mathbf{f} should vanish. Hence the element-by-element absolute value $|(f_i)|$ of the vector \mathbf{f} has to be used. Eq. (13) gives the final results:

$$D_r = |\mathbf{f}^T| d\mathbf{p}, \quad D_m = D_A \tag{13}$$

The interval radius D_r describes the maximum uncertainty of the corrected observations, whereas the interval midpoint D_m is equal to the corrected observation D_A . Using Eq. (1b) and Eq. (2) the interval $[D]$ for the corrected observation can be built:

$$[D] = [D_A - D_r, D_A + D_r] = \langle D_m, D_r \rangle \quad (14)$$

This approximate approach is very useful to analyze the contributions of special influence factors to the whole uncertainty. The strict approach is based on an *interval extension* of the correction models according to Eqs. (9) and (10), cf. Eq. (6).

3.4 Example

Parameter	Uncertainty	Contribution To l_r [mm]
Instrumental-specific: total		1.095
Internal refractive index n_0		≈ 0
-Temperature	$\pm 0.1^\circ\text{C}$	
-Pressure	$\pm 0.05 \text{ hPa}$	
-Relative humidity	$\pm 1\%$	
-Model constants	± 0.5 last digit	
Frequency	$\pm 5 \text{ Hz}$	0.005
Addition constant	$\pm 0.5 \text{ mm}$	0.5
Rounding error	± 0.5 last digit	0.5
Reflector-specific		0.004
-Refractive index of glass BK7 n_p	$\pm 5 \text{ ppm}$	
-Geometric constants d,e	$\pm 0.5 \text{ mm}$	
-Angle of incidence β	$\pm 0.7 \text{ gon}$	
Refractive index n		0.13
-Temperature	$\pm 0.1^\circ\text{C}$	
-Pressure	$\pm 1 \text{ hPa}$	
-Humidity	$\pm 1\%$	
-Model constants	± 0.5 last digit	

Table No. 1. Overview of the magnitude of interval radii

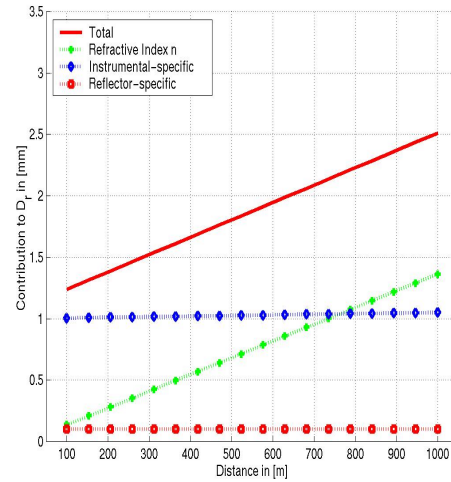


Figure No. 3. Interval radii versus distance

Table No. 1 gives an overview of the contributions of the different effects to the interval radius for a 100m distance. The first column lists the influence parameters whose uncertainty is considered. In the second column, the values are given according to Rüeger (1996) or to manufacturer's information. The third column shows the contribution to the interval radius. The total effect of uncertainty is 1.1mm for the 100m distance, i.e. the sum of rows 1, 10, and 14.

Figure No. 3 shows the behaviour of the interval radius and of the different influence parts due to a variation of the distance from 100m to 1000m . The main contribution factors explained in Table No. 1 are represented here as well. We can distinguish two different characteristics. According to Eq. (11) there exists a first group of influence factors which depends linearly on the distance, i.e. the contribution of the modulation frequency f_0 and the refractive index of the air n . The second group contains the remaining influence factors, i.e. the internal refractive index, the rounding-off errors, the additional constant, and the reflector specific contributions. These second contributions lead just to a constant offset. Finally the superposition of these two groups gives the total impact, which is represented by the interval radius.

The following annotations have to be kept in mind. The impact of the *reflector-specific part* is mainly determined by the disorientation or incidence angle β , cf. e.g. Rüeger (1996, p.161). In this example the incidence angle β is fixed to 30° and the geometric dimensions of the Leica Reflector GPR1 are used, cf. Rüeger (1996, p.257). Hence this influence is constant. The small and constant influence of the instrumental internal reference values is only valid if the Eq. (10) is used. Often the multiplicative relation of Eq.(10) is replaced by an approximate additive one in the sense of a ppm correction.

$$D_A = D_0(1 + n_0 - n) \quad (14)$$

4. Interval extension of least-squares adjustments

Let $E(\mathbf{I})$ be the expectation of the vector of observations \mathbf{I} , \mathbf{A} the configuration matrix, i.e. the matrix of the partial derivations, and \mathbf{a}_0 the zero-order vector of the Taylor expansion. Then a linearized Gauss-Markov model, cf. Koch (1988), is given by:

$$\begin{aligned} E(\mathbf{I}) &= \mathbf{A} \mathbf{d}\mathbf{x} + \mathbf{a}_0 \\ D(\mathbf{I}) &= \sigma_0^2 \mathbf{P}^{-1} \end{aligned} \quad (15a,b)$$

The stochastic model is given by the dispersion matrix $D(\mathbf{I})$ of the observations, where \mathbf{P} denotes their weight matrix and σ_0^2 the a-priori variance factor. Using a pseudo-inverse $(\)^+$, Eq. (16) represents the concept of interval extension of the least-squares estimate, cf. Kutterer (1994, 1995):

$$[\mathbf{d}\hat{\mathbf{x}}] = ((\mathbf{A}^T \mathbf{P} \mathbf{A})^+ \mathbf{A}^T \mathbf{P}) (\mathbf{I} - \mathbf{a}_0) \quad (16)$$

According to Eq. (1), Eq. (16) can be split into a midpoint and a radius part. The zero-order vector \mathbf{a}_0 is considered as point interval vector, i.e. $\mathbf{a}_{0,m} = \mathbf{a}_0$, $\mathbf{a}_{0,r} = \mathbf{0}$.

$$\begin{aligned} \mathbf{d}\hat{\mathbf{x}}_m &= (\mathbf{A}^T \mathbf{P} \mathbf{A})^+ \mathbf{A}^T \mathbf{P} (\mathbf{I}_m - \mathbf{a}_0) \\ \mathbf{d}\hat{\mathbf{x}}_r &= |(\mathbf{A}^T \mathbf{P} \mathbf{A})^+ \mathbf{A}^T \mathbf{P}| \mathbf{I}_r \end{aligned} \quad (17 a,b)$$

The midpoint \mathbf{I}_m is the actual value for the corrected observation vector \mathbf{I} . Eq. (17a) is identical with the classic least-squares estimate, which takes into account the stochastic information about the observations contained in the dispersion matrix $D(\mathbf{I})$. The maximum uncertainty modelled by the interval approach is propagated to the estimates, cf. Eq. (17b).

For geodetic 2d network adjustment, classic quality measures are given by point error or confidence ellipses. The following proceeding can be proposed for the derivation of similar quality measures for the interval approach: The diameters of the intervals described by Eq. (17b) give the uncertainty for each coordinate with respect to the coordinate system chosen for the network adjustment. Hence, an interval inclusion of each point can be built by means of the Cartesian product of the corresponding one-dimensional interval diameters. The resulting boxes are parallel with respect to the coordinate axes and centred at the midpoint, i.e. the estimated point position, cf. Eq.(17a). The areas of the rectangles obtained in the above-explained way can be considered as *quality measures in the interval sense*.

Contrary to the point error ellipse which has the associated confidence probability of 39.4% of overlapping the unknown expectation value, all *possible* positions explained by the interval vector $[\mathbf{I}]$ of the corrected observations are enclosed in the interval boxes.

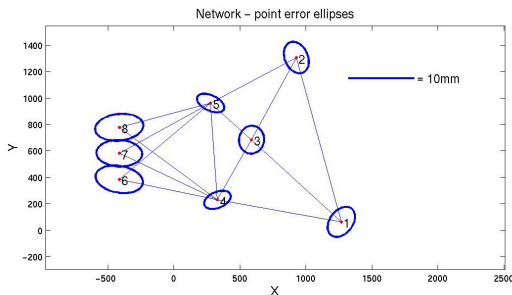


Figure No. 3: Point error ellipses

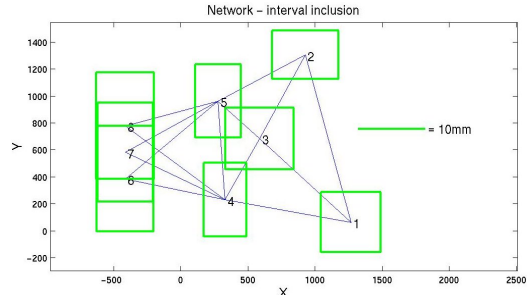


Figure No. 4: Interval inclusion

Figure No. 3 shows the classic point error ellipses for a 2D distance network. The standard deviation of the distances is given by $\sigma = 2mm + 2ppm$. Figure No. 4 depicts the interval inclusion

obtained by Eq. (17b), whereas the uncertainties of the influence parameters are chosen according to Table No. 1.

5. Network Optimization

The classic optimization approaches search to optimize criteria of precision or reliability, cf. Grafarend and Sanso (1985), Kuang (1996). Precision criteria are derived from the covariance matrix of the estimated parameters. Eq. (18) give the example of a pseudo-inverse for free network adjustment:

$$\mathbf{C} = (\mathbf{A}^T \mathbf{P} \mathbf{A})^+, \quad \sigma_{mean} = \sqrt{\frac{tr(\mathbf{C})}{n_{points}}} \quad \text{for } n_{points} \text{ network points} \quad (18)$$

On the one hand, we can distinguish global precision measures, like e.g. the trace $tr(\mathbf{C})$, the mean point error σ_{mean} , or the maximum eigenvalue $\mu = \max(eig(\mathbf{C}))$. On the other hand, criterion matrices which are derived from point error ellipses can be seen as local quality measures. In this paper we use the mean point error as an example for a global precision measure.

For simplicity, the redundancy numbers r_i , i.e. the elements of the vector \mathbf{r} , can be considered as indicators for the reliability of the n_{obs} observations.

$$\mathbf{r} = \text{diag}(\mathbf{I} - \mathbf{A}(\mathbf{A}^T \mathbf{P} \mathbf{A})^+ \mathbf{A}^T \mathbf{P}), \quad r_{mean} = \frac{1}{n_{obs}} \sum_{i=1}^{n_{obs}} r_i \quad (19)$$

The above-introduced interval-based network quality measure suggests to study optimization strategies which take into account these uncertainty effects. Eq. (17b) implies that minimum radii \mathbf{dx}_r for the estimated parameters can be reached by a minimization of the radii of the observations \mathbf{I}_r , or a variation of the configuration matrix \mathbf{A} , or of the observation weights \mathbf{P} . In real applications, the combination of the measurement instruments and the analysis methods determines the values of \mathbf{I}_r and influences \mathbf{P} . As in classic network optimization we can distinguish between a first order design, i.e. a variable matrix \mathbf{A} and a fixed combination of instrument and analysis methods, and a second order design, i.e. with \mathbf{P} and \mathbf{I}_r variable whereas \mathbf{A} is fixed.

In the following, three different free network designs are presented in order to give some idea how changes in the network design can affect the different quality measures. Table No. 2 indicates the used designs and observations.

Design	Measured elements between point i – point j
(1)	Distances: 1-2, 1-5, 1-4, 2-3, 2-6, 2-5, 3-6, 4-5, 5-6
(2)	Distances: Design (1) plus distances 2-4, 3-5
(3)	Distances: Design (2) Directions: 1-2, 1-5, 1-4; 2-3, 2-6, 2-5, 2-4, 2-1; 3-6, 3-5, 3-2; 4-5, 4-1, 4-2; 5-6, 5-4, 5-1, 5-2, 5-3; 6-5, 6-2, 6-3

Table No. 2. Definition of the network designs

Measurements between points	Distance [m]	Standard deviation	Interval radius I_r
Distances			
1-4, 2-5, 3-6	500.0	3.0 mm	1.8 mm
1-2, 2-3, 4-5, 5-6	100.0	2.2 mm	1.2 mm
1-5, 2-4, 2-6, 3-5	509.9	3.0 mm	1.8 mm
Directions		0.5 mgon	0.5 mgon

Table No. 3. Overview of the input data

Table No. 3 gives an overview of the input data: The first column indicates the used observations, where e.g. 1-2 means the observation from point 1 to point 2. In the following columns the values for the distances are given, their standard deviations according to the stochastic model $\sigma = 2mm + 2ppm$. Their interval radii according to Table No. 1 and Figure No. 3 are listed in the next two columns. For the directions both the stochastic model and the interval radii are chosen as 0.5 mgon.

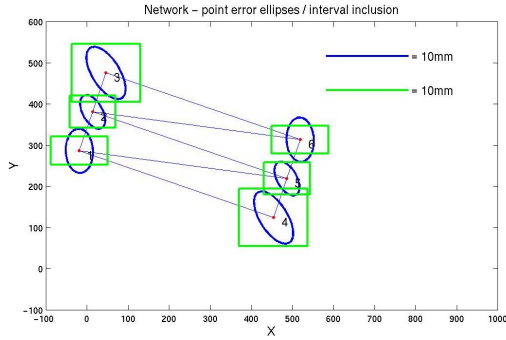


Figure No. 5a. Quality Measures in Design (1)

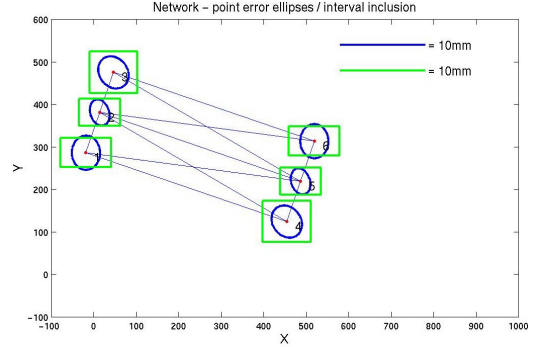


Figure No. 5b. Quality measures in design (2)

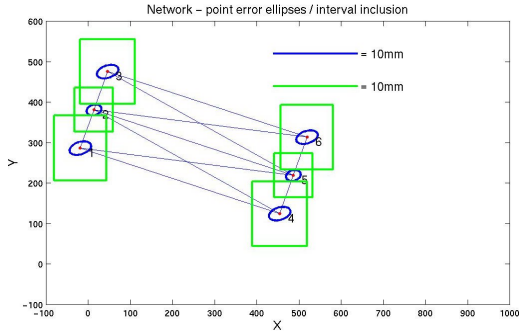


Figure No. 5c. Quality Measures in design (3)

Figures No. 5a-c show the results obtained by Eq. (16) and Eq. (17a). The point error ellipses are depicted in blue (BW reproduction: dark lines), the interval boxes in green (BW: bright lines). Please note that the scale for both quality measures is the same in all figures.

Table No. 4 gives an overview of the numeric results obtained from the different designs, which are indicated in the first column. Both the mean point errors σ_{mean} and the mean redundancy numbers r_{mean} are listed. These global precision and reliability measures are computed with respect to Eq. (18) and Eq. (19). The next columns contain the interval radii x_r and y_r for the coordinates of the six network points obtained by Eq.(17b) and the semimajor (a) and semiminor (b) axis of the point error ellipses.

Design	Point	Interval radius [mm]		Semiaxes of point error ellipses [mm]		
		x_r	y_r	a	b	
(1)	1	3.5	1.7	2.7	1.6	
	2	2.8	2.0	2.2	1.2	
	$r_{mean} = 0$	3	4.2	3.5	3.6	1.7
	$\Sigma_{mean} = 3.2 \text{ mm}$	4	4.2	3.5	3.6	1.7
	5	2.8	2.0	2.2	1.2	
	6	3.5	1.7	2.7	1.6	
(2)	1	3.0	1.7	2.0	1.6	
	2	2.4	1.6	1.6	1.1	
	$r_{mean} = 18\%$	3	2.8	2.4	2.0	1.6
	$\Sigma_{mean} = 2.3 \text{ mm}$	4	2.8	2.4	2.0	1.6
	5	2.4	1.6	1.6	1.1	
	6	3.0	1.7	2.0	1.6	
(3)	1	3.1	4.0	1.3	0.7	
	2	2.3	2.7	0.9	0.6	
	$r_{mean} = 54\%$	3	3.3	4.0	1.3	0.7
	$\Sigma_{mean} = 1.3 \text{ mm}$	4	3.3	4.0	1.3	0.7
	5	2.3	2.7	0.9	0.6	
	6	3.1	4.0	1.3	0.7	

Table No. 4. Comparison of the results

Design (2) completes the network graph of Design (1), cf. Figure No. 5a and Figure No. 5b. This yields smaller and more homogeneous point error ellipses and smaller interval boxes. Furtheron, the reliability is improved, too. Design (1) allows just the determination of the coordinates without any redundancy. The completion of the network graph improves the reliability, e.g. the mean redundancy number is now: $r_{mean} = 18\%$. In Design (3) directions are added as a second type of observations. Hence, the classic precision and reliability criteria, i.e. the point error ellipses and the redundancy numbers can be improved. The mean point error is now $\sigma_{mean} = 1.3 \text{ mm}$ and the mean redundancy number is $r_{mean} = 54\%$. Contrary to these results the interval-based quality criterion shows no further improvement.

This can be explained if different mechanisms are considered during the change of the network design, i.e. the configuration matrix \mathbf{A} . On the one hand, a change of the matrix \mathbf{A} in the sense of addition of observations can improve the algebraic properties of the matrix product

$$\mathbf{U} = (\mathbf{A}^T \mathbf{P} \mathbf{A})^+ \mathbf{A}^T \mathbf{P} \quad (20)$$

or at least of the covariance matrix \mathbf{C} , cf. Eq.(18). Especially effects like

$$|u_{ij}| \geq |u_{ij}^*|, \quad \text{for some } i, j \quad (21)$$

for the change of the configuration from \mathbf{A} to \mathbf{A}^* are important in this context. On the other hand according to Eq. (17b), the addition of further measurements like the directions implicated a larger dimension of the vector \mathbf{l}_r , hence more uncertainty to be propagated to the estimated coordinates. Despite of the addition of observations to the configuration of Design (1) to reach Design (2), all quality criteria are improved. Hence the first mechanism has compensated the uncertainty of the added observations. Comparing Design (2) and Design (3) this is no longer the case. The second mechanism dominates. Hence optimal designs are balancing the extreme results. Then further improvements can only be reached by other combinations of instruments and correction models.

6. Conclusions

In this paper the interval-based description of uncertainty in geodetic measurements was motivated. The presented approach is independent of any random distribution assumptions for information and auxiliary measurements. Hence it seems to be more adequate in those cases when objective and reliable information about the random distribution does not exist. Interval-based uncertainty measures describe maximum effects whereas stochastic approaches lead to average results. This cardinal property is often required in technical applications in order to manage worst-case scenarios. An interval extension of the least-squares estimate allows the propagation of the uncertainty measures to the estimated parameters, i.e. the network coordinates. Further studies have to focus on the application of interval-based uncertainty descriptions to the combination of all observations in a topocentric 3d coordinate system. Eq. (17b) can be used to derive analytical expressions for optimization algorithms. Consequently, network designs are obtainable which fulfil both interval-based and stochastic-based quality criteria.

Acknowledgement

The presented paper shows intermediate results of the research project KU 1250 /1-1 “Optimaler Entwurf geodätischer Überwachungsmessungen unter Berücksichtigung strenger Toleranzen”, which is sponsored by the Deutsche Forschungsgemeinschaft (DFG). This is gratefully acknowledged by the authors.

References

- Alefeld G. and J. Herzberger (1983). *Introduction to Interval Computations*. Academic Press, New York.
- Grafarend E.W. and F. Sansò (1985). *Optimization and Design of Geodetic Networks*. Springer, Berlin Heidelberg New York.
- ISO (1995). *Guide to the Expression of Uncertainty in Measurements*. German translation: Leitfaden zur Angabe der Unsicherheit beim Messen. Deutsches Institut für Normung, Beuth Verlag, Berlin Wien Zürich.
- Koch K.-R. (1999). *Parameter Estimation and Hypothesis Testing in Linear Models* (2d Ed.). Springer, Berlin Heidelberg New York.

- Kuang S. (1996). *Geodetic Network Analysis and Optimal Design*. Ann Arbor Press, Chelsea, Michigan.
- Kutterer H. (1994): Intervallmathematische Behandlung endlicher Unschärfen linearer Ausgleichungsmodelle, DGK C 423, München.
- Kutterer H. (1995). The effect of fuzzy weight matrices on the results of least squares adjustments, In: F. Sansò (Ed.) *Geodetic Theory Today*. IAG Symposium No. 104, Springer, Berlin Heidelberg New York, pp. 224-234.
- Rüeger J.-M. (1996). *Electronic Distance Measurement – An Introduction* (4th Ed). Springer Berlin Heidelberg New York.
- Rüeger J.-M. (1999): Report of the “Ad-Hoc Working Party on Refractive Indices of Light, Infrared and Radio Waves in the Atmosphere” of the IAG SC3. IUGG Birmingham, UK.